Journal of Catalysis 270 (2010) 285–298

Contents lists available at ScienceDirect

Journal of Catalysis

journal homepage: www.elsevier.com/locate/jcat

Activity, durability and microstructural characterization of ex-nitrate and ex-chloride $Pt/Ce_{0.56}Zr_{0.44}O_2$ catalysts for low temperature water gas shift reaction

Arup Gayen [a,1], Marta Boaro [a,*], Carla de Leitenburg [a], Jordi Llorca [b], Alessandro Trovarelli [a]

[a] Dipartimento di Scienze e Tecnologie Chimiche, Università di Udine, via del Cotonificio 108, 33100 Udine, Italy
[b] Institut de Tècniques Energètiques, Universitat Politècnica de Catalunya, Diagonal 647, ed. ETSEIB, and Centre de Recerca en Nanoenginyeria, Universitat Politècnica de Catalunya, Pasqual i Vila 15, 08028 Barcelona, Spain

ARTICLE INFO

Article history:
Received 3 August 2009
Revised 18 December 2009
Accepted 6 January 2010
Available online 9 February 2010

Keywords:
Low temperature water gas shift (LT-WGS)
$Pt/CeO_2–ZrO_2$
Solution combustion synthesis
Incipient wetness impregnation
Ceria
Zirconia
Hydrogen

ABSTRACT

Ex-nitrate and ex-chloride Pt over $Ce_{0.56}Zr_{0.44}O_2$ have been prepared by a single-step solution combustion synthesis (SCS) and are compared with the corresponding catalyst prepared by incipient wetness impregnation (IWI) of platinum over the bare support for the water gas shift reaction under a simulated reformate gas composition. All the catalysts have similar surface areas (23–27 $m^2\,g^{-1}$). Structural and microscopic characterization shows the presence of metallic Pt in all the catalysts. Ex-nitrate catalyst prepared by solution combustion synthesis shows an interesting epitaxial bonding between Pt and the support that has an effect on the WGS activity. It is found that the catalysts prepared by solution combustion method are sensitive to pretreatment atmosphere, with the oxidized catalysts more active than the reduced and as-synthesized catalysts. The impregnated catalysts behave similarly in all the three forms. The stability of these materials under reformate atmosphere at 563 K has also been compared. The catalysts experience different degrees of deactivation related to the method of preparation and the precursors used. Sintering of Pt associated with the formation of carbonate is responsible for the decay of activity (10–12%) in SCS catalysts. For the impregnated catalyst from nitrate precursor, there is no sintering effect, but a strong embedding of Pt by the support reduces the activity (overall loss 34%) together with carbonate formation. The behaviour of the impregnated catalyst from chloride precursor is unusual since it shows an overall gain in activity (8%). The removal of chlorides during durability test and long-term stabilization of Pt crystallize size around 3 nm have been attributed as the controlling factors for this catalyst. Recovery of all the catalysts except the impregnated catalyst from nitrate precursor is found to be reversible.
© 2010 Elsevier Inc. All rights reserved.

1. Introduction

In the last few years, the interest for the water gas shift (WGS) reaction has been growing significantly as a result of the advancements in fuel cell technology, and novel catalyst compositions have been proposed to overcome the limits of the available catalysts [1]. Together with gold [2,3], platinum supported on ceria [4–6], titania [7,8], zirconia [9,10] or mixed oxides of ceria–zirconia [11–13] have been intensively studied, and promising compositions were found. There is a common agreement between the scientific community to recognize that the high activity of these formulations is related to a strong synergism between metal and support [14,15]. In fact, the metal favours the adsorption/desorption of reactants and products as well as the decomposition of intermediates through a spillover mechanism, while the presence of defects and surface oxygen vacancies on the support play a fundamental role in the activation of water. On the other hand, the composition and structure of support can affect the adsorption and catalytic properties of the metal itself as well as the nature of the metal–support interface, where the active sites are mainly located. Therefore, the support is a crucial component of the WGS catalysts, and most of the recent studies prove that the reducibility of support is a key property of the WGS compositions, regardless of the mechanism claimed [16,17]. In particular, with respect to the catalysts supported on bare ceria, platinum showed a higher activity when deposited on ceria–zirconia mixed oxides [11–13] since zirconia promotes the surface and bulk oxygen mobility of ceria, increasing its reducibility [18]. It is worthy to note that in the case of comparison of Pt catalysts on different supports, the greater part of studies do not focus on surface area and dispersion of metal, while it would be necessary to compare catalysts with similar surface areas and similar metal loadings and particle size before drawing any conclusion regarding the impact of the oxide support on WGS activity. Nevertheless, zirconia doping has been found effective in

* Corresponding author. Fax: +39 0432 558803.
E-mail addresses: agayenju@yahoo.com (A. Gayen), marta.boaro@uniud.it (M. Boaro).
[1] Permanent address: Department of Chemistry, Jadavpur University, Kolkata 700 032, India.

0021-9517/$ - see front matter © 2010 Elsevier Inc. All rights reserved.
doi:10.1016/j.jcat.2010.01.007

improving the stability of CeO_2-based catalysts since zirconia contributes to reduce the accumulation of carbonates [18,20], which is one of the main causes of deactivation of these compounds in WGS reaction [21,22]. Despite this, ceria–zirconia mixed oxides have been reported to be unsuitable to stabilize the catalyst against sintering of metal phase under reformate atmosphere [19]. More stable catalysts have been obtained by alloying platinum with rhenium [23,24]; the WGS rate has been correlated with the exposed Pt surface area on the various catalysts, suggesting that metal particle size distribution is also an important parameter [24]. In our recent investigation [25], we have pointed out this aspect, and we found that it is important to improve the dispersion of platinum and its interaction with the support by adopting suitable synthesis approaches. Although the activity and durability of platinum catalysts depend on the method of synthesis, most of the investigations do not focus on the effects of preparation. Platinum catalysts are mainly prepared by wet impregnation of their nitrate or chloride precursors, less often by other methods such as coprecipitation [26] or deposition–precipitation [22]. Recently, the combustion synthesis has been shown to be a good approach to prepare an effective LT-WGS catalyst under hydrogen-rich condition and high CO concentration, but at low space velocities, with potential ability to handle the WGS requirements of fuel processor without the necessity of a high temperature stage [27]. Solution combustions synthesis is a convenient one-step route to prepare pure metal oxides [28] and supported metal oxide catalysts with unusual and interesting properties compared to catalysts prepared by conventional routes [27,29]. It is a versatile and energy-efficient method that involves combustion of an aqueous redox mixture of the metal nitrates (oxidizer) with an organic fuel (reducer). The exothermic nature of combustion process allows high process temperatures self-sustained making it an energetically efficient synthesis. The only external thermal energy requirement is for the dehydration of the fuel/oxidizer precursor mixture and for bringing it to combustion.

We have used this approach to prepare a series of $Pt/Ce_{056}Zr_{0.44}O_2$ catalysts and to investigate their low temperature WGS activity. As support, we choose a solid solution with intermediate Ce/Zr loading because these compositions show optimal redox properties if compared with Ce- or Zr-rich compositions [30–34]. Moreover, for Pt-promoted catalysts, it has been demonstrated that the addition of zirconium atoms into ceria to form binary oxides of composition similar to the one investigated here contributes to a measurable improvement in the water gas shift rate [11]. We have been mainly focused on structural and morphological characterization and on the investigation of WGS activity of catalysts prepared by solution combustion method in comparison to those prepared by conventional wet impregnation, with the aim of testing the feasibility of this approach to prepare noble metal WGS catalysts of increased performance.

2. Experimental

2.1. Synthesis of catalysts

The single-step solution combustion method for the preparation of $Pt/Ce_{0.56}Zr_{0.44}O_2$ catalysts involves combustion of an aqueous redox mixture of the metal nitrates with an organic fuel carbohydrazide at ~623 K. A typical preparation consisted of dissolving $(NH_4)_2Ce(NO_3)_6$ (Treibacher Industrie A.G.), $ZrO(NO_3)_2$ (Aldrich), $Pt(NH_3)_4(NO_3)_2$ (Stream Chemicals) and CH_6N_4O (carbohydrazide, CH) (Aldrich), in the molar ratio 0.56:0.44:0.03:2.22, in a minimum volume of water by slow heating. The amount of Pt was established on the basis of our previous investigation [25], and the amount of carbohydrazide have been calculated by considering the oxidizing and reducing valency of the metal nitrates and the fuel in order to have an equivalence ratio $\Phi_e = 1$ [28]. The solution is then transferred to a preheated muffle furnace maintained at the ignition temperature of about 623 K. Initially, the solution boils with frothing and foaming followed by complete dehydration when the surface gets ignited and burns with a flame yielding a voluminous solid product within a minute. The combustion reaction was vigorous owing to very high heat of combustion when stoichiometric amount of fuel is used, and products flew out of the container. Following previous investigation [28], a fuel lean redox mixture containing half the stoichiometric amount of fuel was used to reduce the exothermicity of the combustion process. From now on, this one-step directly prepared catalyst will be represented as SCS(N). For similar catalyst prepared using the chloride precursor of platinum, $H_2PtCl_6{\cdot}xH_2O$ (Aldrich), 60% of the stoichiometric amount of fuel was used, and the sample was named SCS(Cl). This amount of fuel was chosen in order to obtain an homogeneous combustion and a final product with surface area comparable to that of SCS(N) catalyst. The bare support $Ce_{0.56}Zr_{0.44}O_2$ was prepared by the same method using half the stoichiometric amount of fuel, and it will be named as CZ.

For the preparation of the impregnated catalysts, platinum was deposited by incipient wetness impregnation of the corresponding nitrate or chloride precursors over the bare support CZ. The support was first dried and then impregnated with an appropriate volume of the aqueous solution of Pt precursor, corresponding to the support pore volume. The samples were then dried overnight at 383 K, crushed and calcined at 823 K for 60 min in air flow to obtain the fresh catalysts. The temperature of calcination was established on the basis of previous studies, which have shown that low calcination temperatures are not suitable to obtain active Pt-promoted catalysts [25]. The catalysts impregnated by the nitrate and chloride precursors will be designated as IWI(N) and IWI(Cl), respectively. The metal loading and chloride content was checked by elemental analysis using ICP mass technique. Physico-chemical properties of all the catalysts investigated here together with the bare support have been listed in Table 1.

2.2. Characterization of catalysts

The synthesized materials have been characterized by XRD, BET and HRTEM. X-ray powder diffraction patterns were collected in a Philips PW3040/60 X'pert PRO diffractometer (equipped with an X'celerator detector) operated at 40 kV and 40 mA, using Ni-filtered Cu Kα radiation in the 2θ range 20°–100° with a step size of 0.02° and a counting time of 80 s per step. Profile analysis of XRD patterns was carried out by Rietveld refinement using GSAS-EXPGUI program [35,36].

The BET surface areas were measured in a TriStar3000 surface area analyzer (Micromeritics). Before each measurement, the samples were degassed at 423 K in vacuum for 60 min.

Table 1
Physico-chemical properties of the catalysts.

Name of catalyst	Pt (wt.%)[a]	Cl (wt.%)[a] [AP]	Cl (wt.%)[a] [aged]	Surface area ($m^2\ g^{-1}$)	Pt size[b] [fresh]	Pt size[c] [aged]
CZ				26		
SCS(N)	4.41			27	2.2–4.5	2.8–6.0
SCS(Cl)	4.82	0.43	0.18	23	2.0–4.4	2.4–6.0
IWI(N)	4.18			26	3.2–5.2	2.8–5.2
IWI(Cl)	4.17	0.60	0.30	27	1.6–3.6	2.0–4.4

[AP] = as-prepared catalyst; [fresh] = SCS catalysts in oxd773 form and impregnated catalysts in as-prepared form; [aged] = catalysts after durability test.
[a] From ICP analysis.
[b,c] From HRTEM analysis.

Microstructural characterization by High-Resolution Transmission Electron Microscopy (HRTEM) was performed at an accelerating voltage of 200 kV in a JEOL 2010F instrument equipped with a field emission gun. The point-to-point resolution was 0.19 nm, and the resolution between lines was 0.14 nm. The magnification was calibrated against a Si standard. No induced damage of the samples was observed under prolonged electron beam exposure. Samples were dispersed in alcohol in an ultrasonic bath, and a drop of supernatant suspension was poured onto a holey carbon-coated grid. Images were not filtered or treated by means of digital processing, and they correspond to raw data. More than 200 individual particles were analyzed for the determination of particle size distribution. Temperature-programmed desorption (TPD) in He (35 ml min^{-1}) of the catalyst samples was carried out in a Micromeritics AutoChem II 2920 instrument. After flushing in He (50 ml min^{-1}) at RT for 30 min, the temperature was ramped (10 K min^{-1}) from RT to 1073 K. The liberated gases were simultaneously analyzed using an online quadrupole mass spectrometer (OmniStar, Pfeiffer Vacuum).

The Pt dispersion was determined by dynamic CO chemisorption method in pulsed mode in the same apparatus where TPD experiments were performed. A 3.95% CO/He gas mixture was used. Before each chemisorption measurement, the sample was degassed in He (50 ml min^{-1}) at 473 K for 15 min followed by reduction in 4.93%H_2/Ar (35 ml min^{-1}) for 15 min (except when the catalyst was pre-reduced) and then cooled in He (35 ml min^{-1}) to 323 K. Once a stable baseline is established, the 3.95% CO/He (35 ml min^{-1}) mixture was pulsed from a calibrated loop (5 ml) kept at 383 K and ambient pressure, into the He flow until the consecutive TCD peaks were equal in size. Chemisorption study over pure support was also carried out in a similar manner.

2.3. Catalytic test

The steady-state water gas shift activity was studied in a plug flow quartz microreactor (16″ length, and 0.25″ ϕ, internal diameter) over 0.170 g of catalyst between 473 and 603 K. The operating conditions were chosen to simulate those existing in a LT-WGS reactor for fuel processing with an inlet feed composition of 36%H_2, 26%N_2, 7%CO, 10%CO_2 and 21%H_2O and a space velocity of 40,000 h [37]. The water was delivered with a precision syringe pump, and the line before and after the reactor was kept at 473 K by heating tapes to avoid condensation. The temperature was increased at 10 °C/min from 473 K to 603 K in five steps. A bypass line was included in the layout to measure directly the composition of the dry inlet feed. At every temperature, the reactants and products were monitored every 1.57 min for a total time of 25 min; less than 1% variation on CO conversion was obtained in this time window. The conversion was calculated by averaging the results of the last five chromatograms. The durability tests were carried out at 563 K by monitoring the outlet gases every 1.57 min. The water was condensed before entry to the micro-GC analyzer by a refrigerator and quantified indirectly from the changes in the total flow rate using nitrogen as internal standard. A Varian CP4900 micro-Gas Chromatograph (micro-GC) equipped with three columns was used; one molecular sieve column (MS, carrier N_2) for the detection of H_2, another MS column (carrier He) for CO and N_2, and a Poraplot Q column (PPQ, carrier He) for the detection of CO_2 and CH_4. Conversion was calculated using the following formula $X_{co} = ((CO_{in} - CO_{out}/\beta/CO_{in})$, where CO_{in} indicates the concentration of CO fed into reactor, CO_{out} indicates the concentration of CO measured at the outlet of the reactor after water condensation, β is a factor that takes in account the change of total flow due to the condensation of water, and it is defined as $\beta = N_{2out}/N_{2dry}$ where N_{2out} is the concentration of N_2 measured at the outlet of the reactor after condensation of water and N_{2dry} is the concentration of N_2 in the dry feed (without water) measured bypassing the reactor and the water syringe pump. From reproducibility tests on samples of the same batch/different batches of catalysts, we can estimate an error of ±3 K (same batch) and ±5 K (different batches) in the conversion-temperature curves.

The equilibrium conversion was calculated using the package software HSC5.1 (Outokumpu). The shift activity was evaluated on the following states of the catalysts.

1. *AP*: The catalyst was tested in its as-prepared form.
2. *Red773*: The as-prepared catalyst was reduced in situ in 5%H_2/N_2 at 773 K for 60 min from RT at 10 K min^{-1}, cooled to 473 K in the same flow, degassed in N_2 for 15 min followed by switch over to the WGS feed atmosphere.
3. *Oxd773*: The as-prepared catalyst was oxidized in situ in air at 773 K for 60 min from RT at 10 K min^{-1}, cooled to 473 K in the same flow, degassed in N_2 for 15 min followed by switch over to the WGS feed atmosphere.
4. *Aged*: Fresh catalyst sample pretreated as oxd773 that has undergone a cycle of WGS is cooled in N_2 to RT and is followed by a steady-state durability test at 563 K in the WGS feed atmosphere for about 45 h and finally cooled in N_2 to RT. The shift activity of this catalyst was tested under this heading. The purpose of this test was to understand the extent of deactivation that has happened to the catalyst during the course of durability test.
5. *Regenerated*: After a cycle of WGS over the aged catalyst as discussed above, the catalyst was cooled in N_2 to RT and was then regenerated by oxidizing in situ in air at 773 K for 60 min, cooled to 473 K in the same flow, degassed in N_2 for 15 min followed by switch over to the WGS feed, and the activity was tested. The purpose was to know whether the aged catalyst can be recovered completely through oxidation at 773 K or not.

3. Results

3.1. Textural properties of materials

Fig. 1 shows the powder XRD patterns of the four catalysts and that of the support. All these materials crystallize in the form of solid solution of ceria–zirconia with no evident peak splitting due to the presence of mixed oxide phases. It is very well known that the structural characteristics of ceria–zirconia are strongly dependent on method of synthesis and treatments [38]. At ceria-rich composition, ideal fluorite type structure is preferred, while displacement of oxygen from the ideal fluorite position is observed on increasing Zr content with formation of metastable phases of cubic and tetragonal symmetry. The intermediate composition range is critical since both phases could co-exist and transition from one structure to another may be critically influenced by several parameters [39]. Due to the low scattering factor of oxygen, XRD is not sensitive to these small displacements and in this composition range, it could be difficult to obtain a reliable phase distribution, especially when crystallinity of samples is not high. In our case, the Rietveld analysis of the diffraction profile of the support has been carried out by opening the fitting to cubic, tetragonal and a mixture of the two. Results agree better the presence of a tetragonal phase with $a = b = 3.751(1)$ Å and $c = 5.364(1)$ Å (Table 2). Platinum is dispersed in finely dispersed metallic state over SCS samples as can be seen from the broad metal peaks. The Pt crystallite size determined from XRD line broadening using Scherrer's equation is ca. 4 nm for SCS(N) and 6 nm for SCS(Cl) catalyst. Impregnated catalysts show a narrow Pt(1 1 1) signal indicating the presence of larger crystallites (ca. 50 nm for IWI(N) and 70 nm for IWI(Cl)). Due to the different intensity of the signals in the IWI samples, it is likely that the

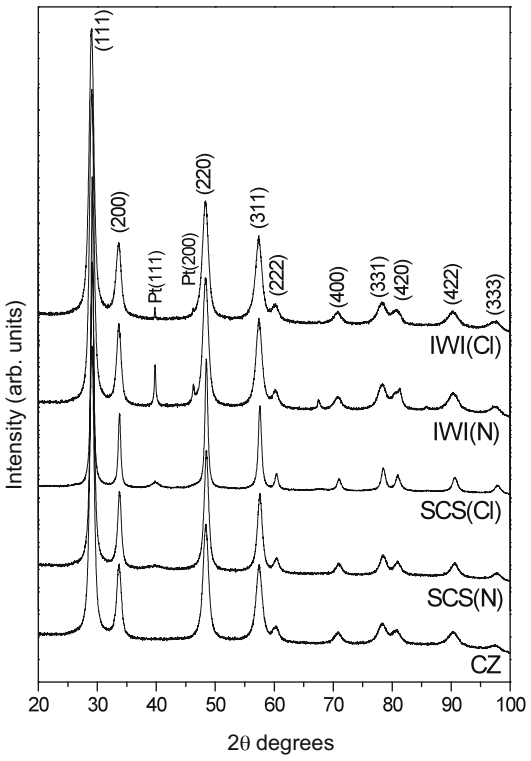

Fig. 1. Powder XRD patterns of the support and the catalysts.

estimate of crystallites size is probably affected by the presence of a few large crystallites of Pt, and it does not represent the real dispersion of metal. Indeed, dispersion data obtained by HRTEM (Table 1) are more in agreement with those measured by XRD in the case of SCS samples, but values obtained for IWI sample strongly differ. This issue will be further addressed in Section 4.

All the materials have similar surface area ranging around 26–27 $m^2\ g^{-1}$ (see Table 1) apart from the SCS(Cl) that has a lower surface area of 23 $m^2\ g^{-1}$. After impregnation of the support with platinum precursors, the surface area remains essentially unaltered.

3.2. Catalytic studies

The WGS activity was investigated under different pretreatment conditions of the catalyst that include AP (as-prepared), red773 (reduced in 5%H_2/N_2 at 773 K for 60 min) and oxd773 (oxidized in air at 773 K for 60 min) to know about the sensitivity of the catalyst state towards a reducing/oxidizing atmosphere. The shift activities of the four catalysts after the above pretreatments are shown in Fig. 2 together with the expected equilibrium conversion. It is found that the SCS catalysts behave differently on the basis of their starting form, and the reactivity follows the order oxd773 > red773 > AP irrespective of the type of platinum precursor employed. For a particular state of the catalyst, the one from nitrate precursor shows higher activity than the one from chloride precursor up to temperatures close to the equilibrium value. On the other hand, the impregnated catalysts showed similar activity in all the three forms except for the as-prepared catalyst using the chloride precursor, which showed a slightly lower activity compared to the corresponding oxidized and reduced catalysts. Unlike the SCS catalysts, the IWI catalyst from chloride precursor has a higher activity in red773 and oxd773 forms compared to its nitrate analogue. Based on these findings, we decided an oxidative pretreatment at 773 K (oxd773) as the standard activation step for further investigations over all the catalysts studied here, in order to compare catalysts in their optimal form.

Fig. 3 compares the activity of the oxd773 catalysts only from the two precursors employed. The SCS catalyst from nitrate precursor is superior to the corresponding IWI catalyst. The activity of SCS(N) is also higher than that of the SCS and IWI catalysts from chloride precursor. Both the catalysts from chloride precursor, on the other hand, show similar activity. All the three catalysts except IWI(N) reached the equilibrium conversion at around 580 K.

To examine the durability of the present catalysts under steady-state conditions, we studied their activities in the same reformate composition at 563 K for about 45 h. Fig. 4 shows CO conversion as a function of time on stream at 563 K for all the four catalysts together with the equilibrium conversion value. The long-term activity pattern follows the following order: IWI(Cl) > SCS(Cl) ≈ SCS(N) ≫ IWI(N). Both the SCS catalysts behave quite similarly. There is an initial decay in activity of ca. 10–12%, and the activity remains essentially constant afterwards. The SCS(Cl) catalyst acquires the stable conversion value faster (in about 5 h) than the SCS(N) catalyst (in about 10 h). The activity of IWI(N) catalyst decreases continuously from an initial value of 66% to a value of 44% after 45 h on stream, indicating an overall loss of 34%. Over this catalyst, a loss of 12% occurs during the first 3 h. The WGS activity over IWI(Cl) increases with time on stream; this is a rather unusual behaviour, and to our knowledge, it has not been reported in the literature so far. In order to verify the reproducibility of this behaviour, the test was repeated on another sample of catalyst of similar composition (Fig. 4, samples 1 and 2). The initial conversion is 74% and increases to about 77% in a first stage (7 h), then it remains constant up to 22 h followed by a second increase up to 32 h when a final conversion of 80% is measured, indicating an overall gain of around 8%. This conversion value is close to the expected equilibrium conversion of 86% at 563 K.

After ageing the catalysts in the WGS atmosphere for 45 h, the catalysts were cooled to room temperature and subjected to a cycle of WGS. Then, they were regenerated by in situ oxidation under air at 773 K for 1 h, and their shift activities have been tested again in a WGS cycle. Fig. 5 compares the shift activity of the aged (after durability test) and regenerated forms of each catalyst to that of the oxd773 catalyst along with the equilibrium conversion expected. Except for the IWI(Cl) catalyst, all the other three catalysts experience a decay in activity during the course of the steady-state durability test in agreement with the observations made from Fig. 4; for the IWI(Cl) catalyst, the activity of the aged form is higher than that of the oxd773. The activity of SCS(N) can be recovered

Table 2
Cell parameters and particle size (PS) for the different materials obtained by Rietveld refinement.

Sample	R_{WP}	R_F^2	X^2	PS CZ (Å)	Cell parameter CZ (Å)		Cell parameter Pt (Å)
					$a = b$	c	$a = b = c$
CZ	5.0	4.0	3.3	188	3.7509 (2)	5.3637 (6)	–
SCS(N)	4.3	2.7	2.1	232	3.7519 (2)	5.3597 (4)	3.932 (4)
SCS(Cl)	4.6	4.3	2.8	395	3.7499 (3)	5.3622 (3)	3.920 (1)
IWI(N)	5.2	3.6	3.7	188	3.7508 (2)	5.3617 (6)	3.9220 (3)
IW(Cl)	4.3	3.7	2.4	170	3.7520 (2)	5.3652 (6)	3.9224 (4)

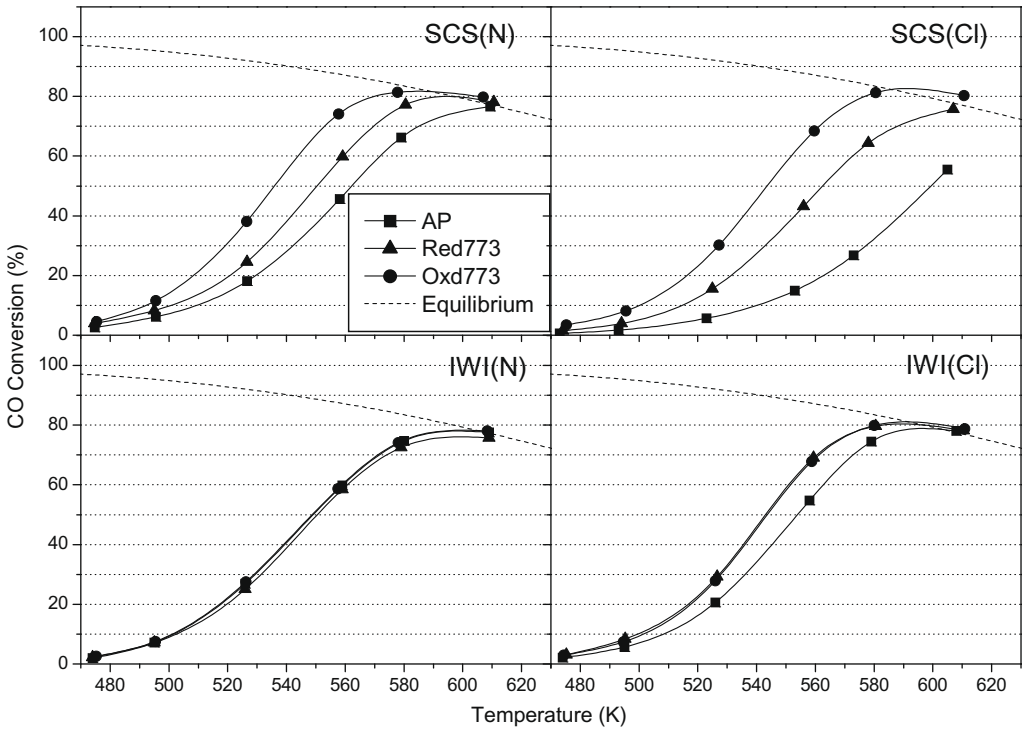

Fig. 2. CO conversion vs. temperature: effect of pretreatment over IWI and SCS samples.

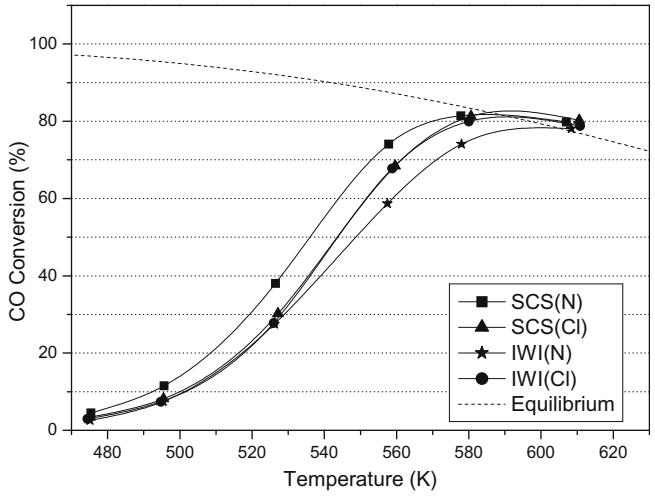

Fig. 3. CO conversion vs. temperature: activity of catalysts after an oxidative treatment under air at 773 K for 1 h.

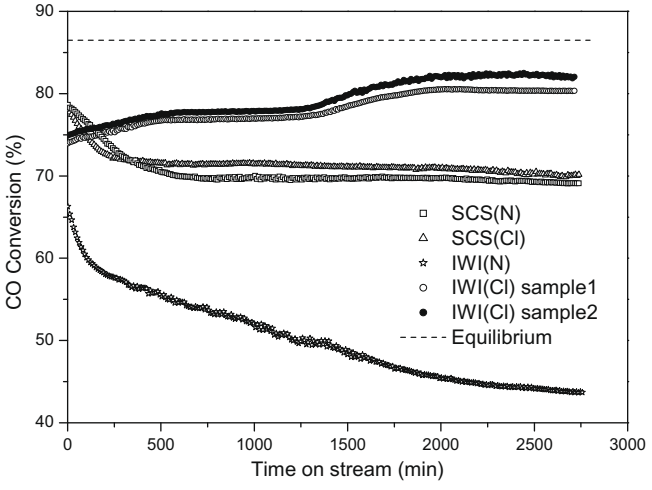

Fig. 4. CO conversion against time in durability tests at 563 K over SCS and IWI catalysts.

completely after regeneration, but this is not true for the corresponding impregnated catalyst, IWI(N), which remains in a permanently deactivated state. The decrease in activity after ageing of the SCS(Cl) can be also recovered completely, while IWI(Cl) catalyst following regeneration procedure exhibits even higher WGS activity than after durability tests.

The possible causes of deactivation can be (a) sintering of platinum that may occur during long-term exposure to the simulated WGS atmosphere, (b) embedding of platinum by the reduced support oxide that eventually decreases the fraction of accessible active site surfaces for CO adsorption and (c) carbonate formation that blocks the active site at the interface region. We have correlated the different sensitivities of the catalysts through (1) microstructural characterization before and after ageing by high-resolution transmission electron microscopy as well as by (2) measurement of platinum dispersion over different forms of catalysts through dynamic CO pulse chemisorption measurements and by (3) TPD in He.

3.3. HRTEM studies

Detailed microstructural characterization by HRTEM can provide powerful information about the nanostructure of the oxide, metal promoter and their interface region [40,41], which can help explaining the stability pattern of the different catalysts. In the following sections, we investigate by HRTEM the structure of each

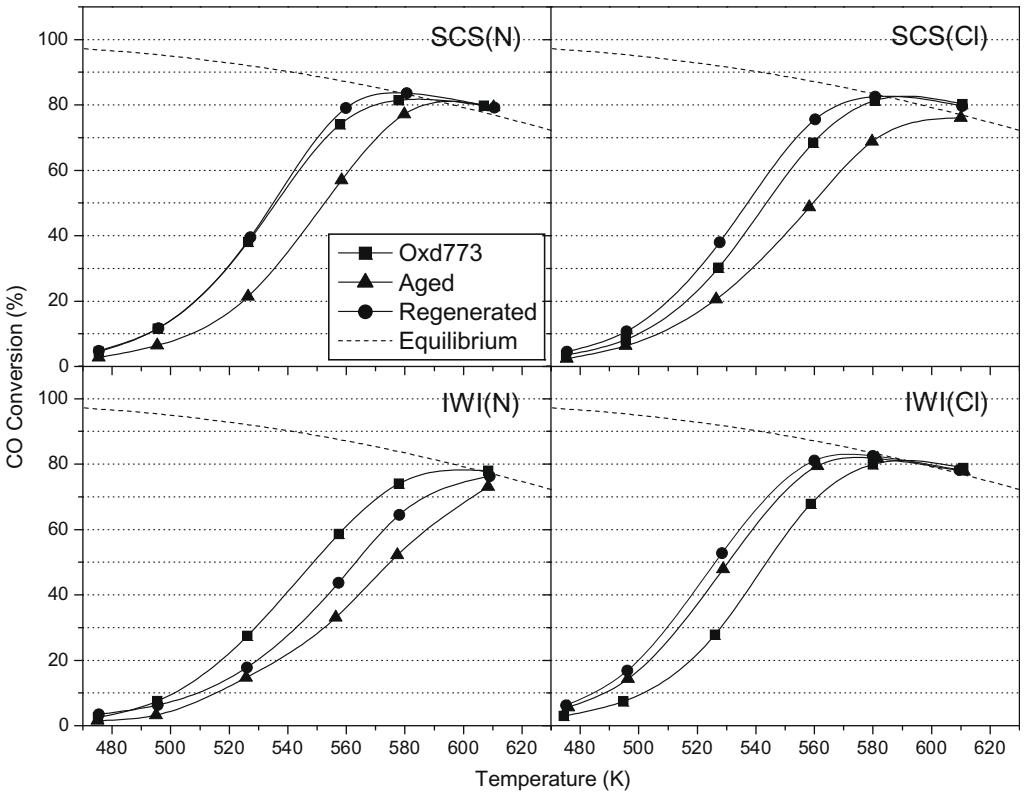

Fig. 5. CO conversion vs. temperature: effect of ageing (45 h under feed composition) and regeneration (1 h in air at 773 K) over SCS and IWI samples.

catalyst before and after the ageing process. In addition, we have also studied the microstructure of the SCS catalysts in their as-prepared and reduced form due to their different behaviour in WGS. The HRTEM results were also supported by CO chemisorption and TPD studies.

3.3.1. SCS(N)

Fig. 6a shows general views of the sample pretreated as oxd773, i.e., before WGS test, at two different magnifications over the same area. The low-magnification part shows the presence of a large number of particles on the support, with excellent dispersion. The support contains both well-faceted and round-shaped crystals from ca. 10–30 nm in size. The diameter of particles is very homogeneous and ranges from 2.2 to 4.2 nm, being centred at about 3.6 nm. When the indicated portion of the low-magnification image was magnified further, together with the metal particles (indicated by white arrows), some void areas (indicated by black arrows) of the CZ support becomes visible. The existence of voids on ceria-based catalyst has been already reported [42]. The amount of voids in the support is surprisingly high and can be probably related to the preparation method. The voids exhibit clear geometric features (hexagonal and triangular) and range from 1.7 to 3.9 nm. Fig. 6b corresponds to a lattice-fringe image of a single particle at high magnification. Lattice-fringes at 3.05 Å correspond to (1 0 1) planes of the CZ support, and spots at 1.96 Å are due to (2 0 0) planes of metallic Pt. Therefore, it appears that the sample is comprised of Pt nanoparticles. In addition, the edges of the Pt particles do not suggest any significant oxidation, that is, there is no oxide layer around.

After ageing in the reformate for 45 h, the SCS(N) sample still contains well-dispersed Pt crystallites, but the distribution of Pt particle size has broadened with respect to the sample before WGS. Now, the mean Pt particle size is between 2.8 and 6.0 nm, being centred at about 4.1 nm. The Pt particle size distribution for both these samples (before and after WGS) is included in Fig. 7 for comparison. Fig. 6c shows representative low-magnification HRTEM images of the aged sample. The ceria–zirconia support maintains its original morphology and size as clear from the low-magnification images. No voids were identified in the aged sample. Fig. 6d shows a characteristic lattice-fringe HRTEM image obtained at high magnification. A single Pt particle (indicated by the square) is enlarged and characterized by lattice spacing at 1.96 Å, which corresponds to Fm3m (2 0 0) planes of metallic Pt. Only metallic Pt is present in the sample besides the CZ support.

3.3.2. SCS(Cl)

The oxd773 sample of this catalyst is comprised of small Pt particles, very well distributed over the CZ support as observed under low-magnification view of this sample (not shown). Particles range from 2.0 to 4.4 nm, and the mean particle size is centred at 3.3 nm (see Fig. 7). This is slightly less than that of the sample prepared from nitrate precursor (3.6 nm). Fig. 6e corresponds to a HRTEM image showing several Pt particles. One of them is indicated by the square, and its corresponding FT image is enclosed. Spots at 2.27 Å correspond to (1 1 1) crystallographic planes of metallic Pt.

Fig. 6f depicts a representative HRTEM image of the sample after ageing. The Pt crystallites remain in a well-dispersed state. However, the particles have increased their size and now ranges from 2.4 to 6.0 nm (see Fig. 7). The final mean particle size, 4.0 nm, is very close to that observed in the aged sample prepared from nitrate precursor (4.1 nm), but the particle size distribution broadness is higher. Lattice-fringe image of a single Pt crystallite and its associated FT image are shown in the insets. Spots at 2.27 Å are ascribed to (1 1 1) crystallographic planes of Pt.

3.3.3. IWI(N)

Since the preparation step of the impregnated catalysts involves calcination at 823 K in air and also because the as-prepared,

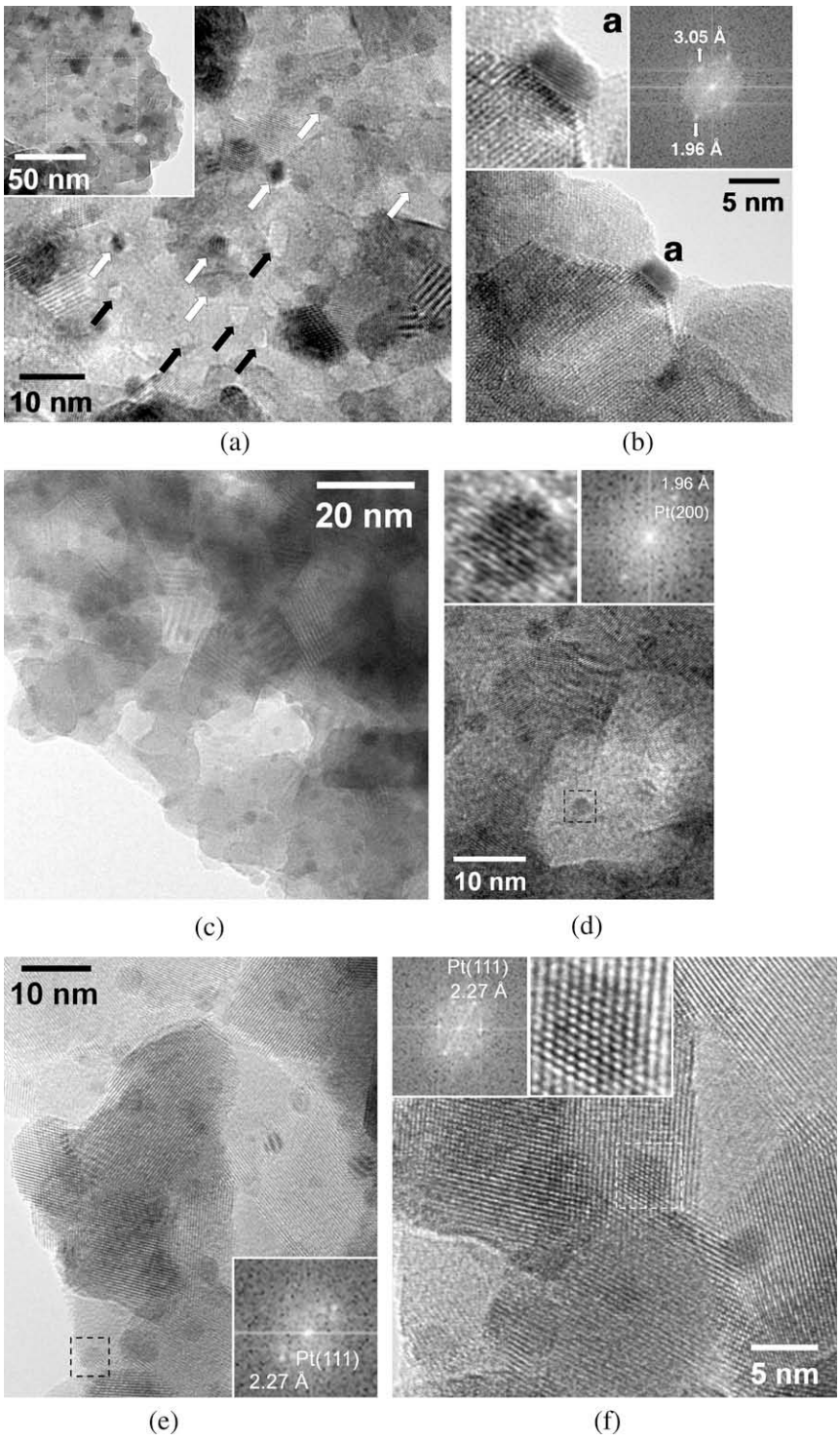

Fig. 6. HRTEM images of (a and b) oxd773. (c and d) aged catalysts of SCS(N), (e) oxd773, and (f) aged catalysts of SCS(Cl).

oxd773 as well as red773 pretreated catalysts show similar shift activity, the HRTEM study was performed over the as-prepared catalysts, and they correspond to the catalyst state before WGS test. Fig. 8a shows high-resolution image of the IWI(N) catalyst before WGS. Numerous Pt particles of about 3.2–5.2 nm in diameter are encountered, being the mean particle size 4.2 nm (see Fig. 7). Particles enclosed in squares *a* and *b* are shown enlarged along with their FT images. In both cases, lattice spacings at 2.27 Å are characteristic of Pt(1 1 1) planes. Spots at 3.05 Å in the FT image of particle *a* correspond to (1 1 1) crystallographic planes of the CZ support. The morphology and size of support crystallites were similar to the SCS catalyst.

Fig. 8b shows representative HRTEM image of IWI(N) aged in the reformate for 45 h. It is constituted by well-dispersed Pt ensembles with a particle size distribution between 2.8 and 5.2 nm, being centred at 4.1 nm (see Fig. 7). It is interesting to note that the Pt particle size distribution is exactly maintained after WGS, in terms of both mean value and broadness, so the decrease

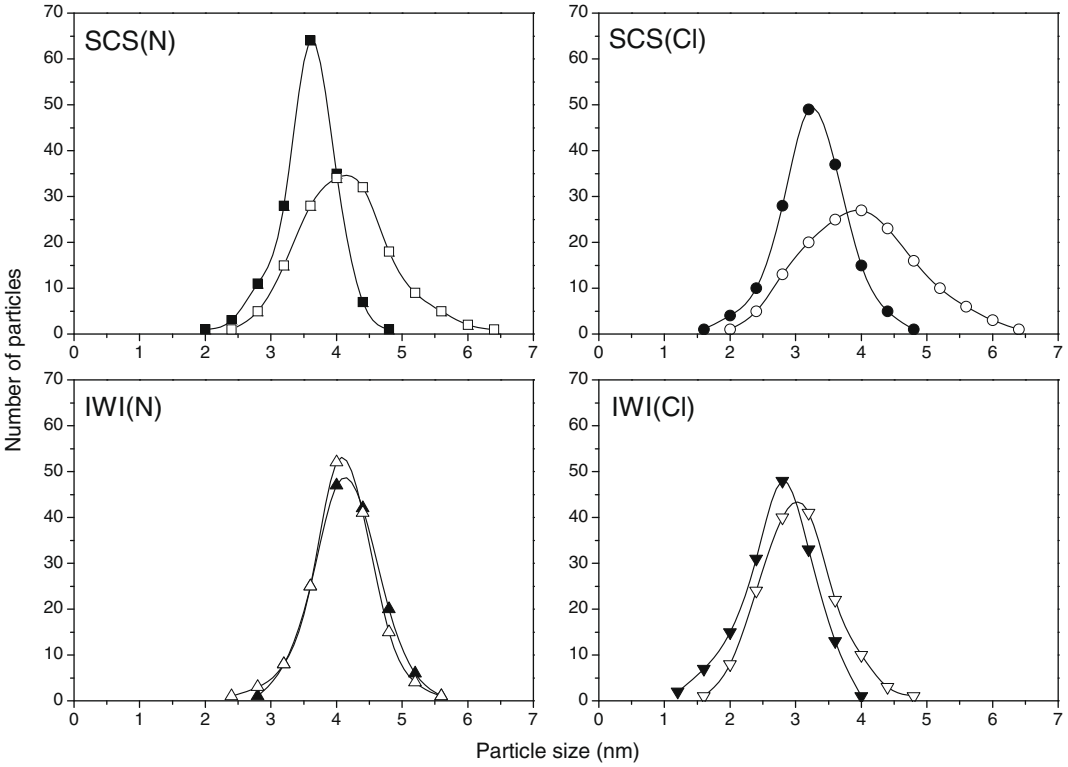

Fig. 7. Distribution of Pt particles over the catalysts from HRTEM analysis for the fresh (■) and aged catalysts (□).

in catalytic activity cannot be related to a sintering effect. The inset images in the figure show a Pt particle exhibiting lattice-fringes and its associated FT image. The Pt particles are not faceted and hardly exhibit lattice-fringes in this sample, suggesting that they could be strongly embedded in the support.

3.3.4. IWI(Cl)

Fig. 8c shows a general view of the sample before WGS, which contains very small Pt crystallites, from 1.6 to 3.6 nm. The Pt particle size distribution is quite narrow and centred at about 2.7 nm (see Fig. 7). Fig. 8d shows a HRTEM image, where a single Pt particle in profile view is enlarged and analyzed by FT. The particle is well faceted. However, it is so small that only a few crystallographic planes can be seen in the lattice-fringe image. The spacing of these lattice-fringes is around 2.2 Å, which is ascribed to (1 1 1) crystallographic planes of Pt. Spots at about 3.1 Å correspond to (1 1 1) planes of the CZ support.

The Pt particle size distribution for the sample after ageing is very close to that of the sample before reaction. Now, Pt particles range from 2.0 to 4.4 nm, with a mean Pt size distribution of 3.0 nm (see Fig. 7). Interestingly, the Pt particle size distribution after WGS has not broadened with respect to the fresh sample (in a similar way to what has been reported above for sample IWI(N)). This is markedly different from both the SCS catalysts, where a broad and large size distribution is observed as discussed above. Fig. 8e shows a general view of the sample, where well-dispersed Pt particles are distributed all over the CZ support. Fig. 8f corresponds to another HRTEM image. The particle enclosed in the square shows spots in the FT image at 2.27 Å, corresponding to Pt(1 1 1).

3.3.5. Microstructure of the AP and red773 SCS catalysts

General microstructural views of the as-prepared and red773 samples of the SCS catalysts are similar to that of the oxd773 samples as discussed above with the average size of platinum being centred at about 3.8 nm, slightly higher than the oxd773 catalysts. The CZ support maintains its original morphology. In addition, the red773 catalyst from nitrate precursor also contains huge amount of voids in the CZ support, which range from 1.0 to 2.3 nm. A comparison between the samples after oxidation or reduction treatments indicates that the number of voids is larger in the reduced sample and that they are significantly smaller. No voids were detected in SCS(Cl) catalyst in any form.

Fig. 9a is a detailed lattice-fringe image of the as-prepared SCS(N) sample, showing that Pt particles and the support likely maintain an epitaxial relationship. First of all, it should be highlighted the excellent homogeneity in Pt particle size (all of the particles exhibit a diameter of 3.8–3.9 nm) and dispersion. Several Pt particles in the image are labelled as "a", "b" and "c", and a single CZ support particle in the center of the image depicts (1 0 1) planes at 3.06 Å, as expected. Insets correspond to FT images of particles "a–c" as well as enlarged lattice-fringes insets of particles "a" and "b". The FT image recorded over the image containing Pt particle "a", for example, shows spots aligned in the same direction. These spots originate from (1 0 1) planes of CZ at 3.06 Å, from (1 1 1) planes of Pt at 2.26 Å and Moiré patterns. The alignment of the spots strongly suggests epitaxy of Pt particles over the CZ support. In addition, there is a regular extinction pattern in the enlarged lattice-fringe image due to a mismatch between the crystal lattices of the CZ support and the Pt nanoparticle, providing an additional evidence for an epitaxial relationship. This is the origin of the Moiré spots in the FT image. Exactly the same situation is encountered in particle "c". The FT image of particle "b" also exhibits aligned spots, but in this case, the alignment is between (0 0 2) planes of CZ at 2.64 Å and (2 0 0) planes of Pt at 1.96 Å. Again, the alignment of spots and the existence of a regular extinction pattern are indicative of epitaxial growth.

The Pt nanoparticles in the reduced sample of SCS(N) also maintain an epitaxial relationship with the support. The high-resolution image in Fig. 9b allows a direct determination of the epitaxial rela-

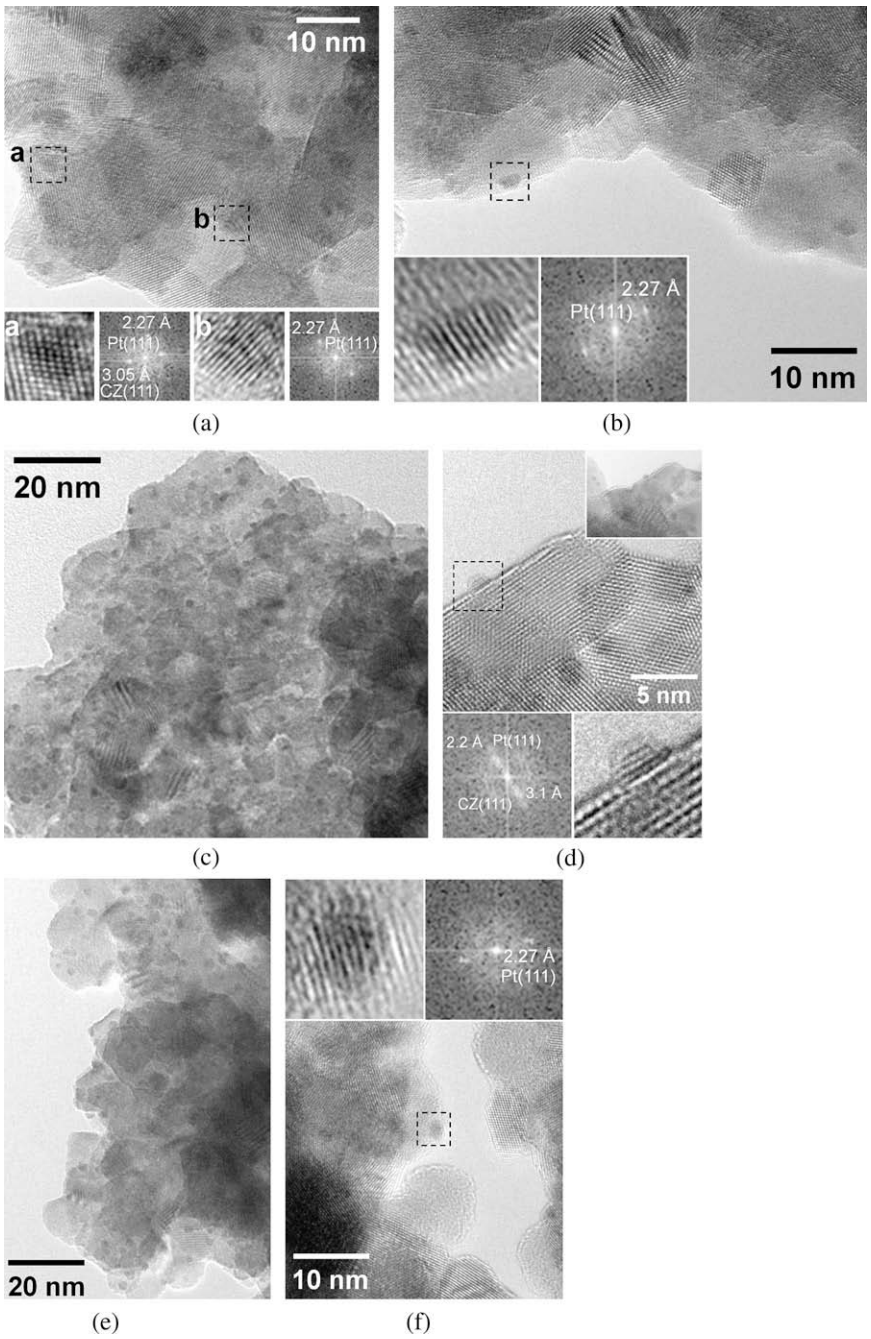

Fig. 8. HRTEM images of (a) oxd773 and (b) aged catalysts of IWI(N); and (c and d) oxd773 and (e and f) aged catalysts of IWI(Cl).

tionship. Crystallographic planes at 3.06 Å corresponding to (1 0 1) planes of the CZ support are aligned parallel to planes at 2.25 Å corresponding to (1 1 1) planes of Pt, as it is also observed in the FT image. In the enlarged image, the periodicity of the epitaxy is found to be 2:3. The match, however, is not perfect, and the periodicity fails after several periods.

The presence of an epitaxial relationship between platinum nano-crystallites and ceria–zirconia support in the as-prepared and red773 forms of SCS(N) catalyst results in stressed particle-support interfaces. But the oxd773 form that shows the highest activity of all the three forms does not show any such epitaxy in the structure. Although enough care is taken to look into its occurrence, the possibility of this kind of structural feature cannot be ruled out. We can only say that even if they are present in the structure, they are statistically insignificant. This unique structural feature might have implications for the observed shift activity pattern.

The HRTEM images of the SCS(Cl) catalyst in as-prepared and red773 forms are shown in Fig. 9c and d, respectively. They look quite heterogeneous than other samples from the Pt crystallite size distribution point of view, and it falls in the range 2–7 nm. It is interesting to note that there is indeed no epitaxial relationship between Pt crystallites and the support or any geometric voids in all the three forms of this catalyst. Thus, reason behind the differences in activity of the as-prepared and red773 catalysts of SCS(Cl) to that of the oxd773 catalyst is of different origin unlike the one we have discussed above for the SCS(N) catalyst.

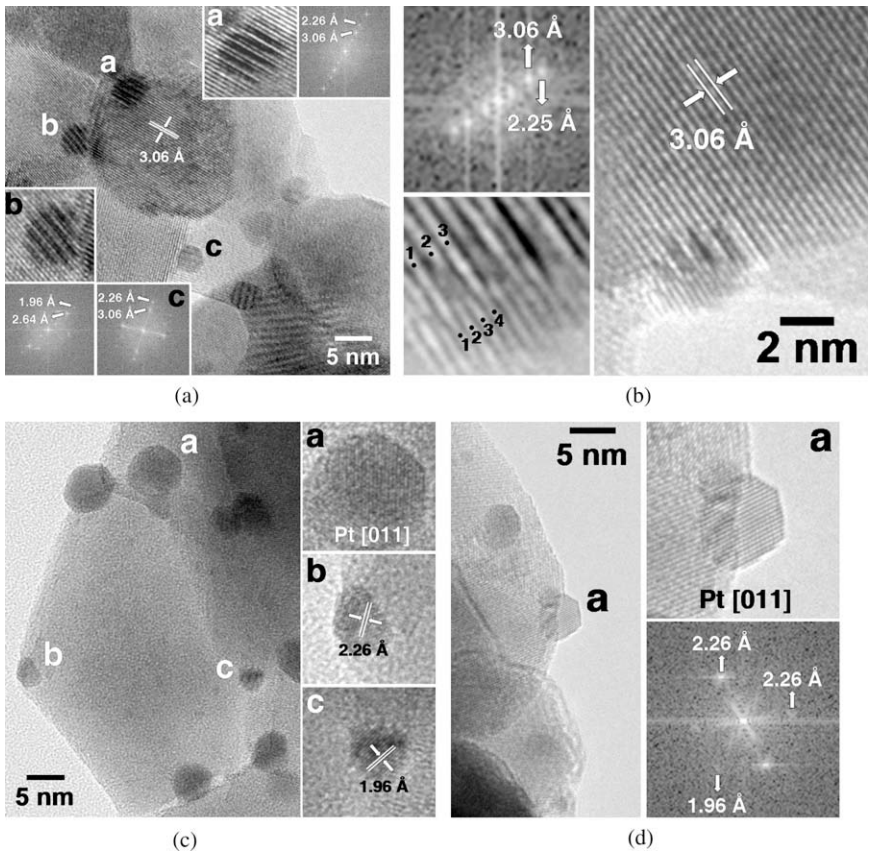

Fig. 9. HRTEM images of the as-prepared and reduced catalysts of SCS(N) (a and b) and SCS(Cl) (c and d).

3.4. CO chemisorption studies

The CO chemisorption measurements have been carried out in order to evaluate the dispersion of platinum before WGS tests (Fig. 10a) and after durability tests (Fig. 10b and c). Therefore, the experiments have been performed under different pretreatment conditions and over different states of the catalysts. The dashed line in Fig. 10 corresponds to treatments during the course of WGS test in the reaction set-up, and the solid line corresponds to treatments associated with the chemisorption measurements in the equipment. Fig. 10a shows the in situ treatments of the catalysts to evaluate the Pt dispersion of fresh catalysts (AP: as-prepared, Ch_{AP}), reduced (red773: reduced in situ in 4.93%H_2/Ar at 773 K for 60 min from RT at 10 K min^{-1} and cooled in the same flow to 473 K, Ch_{RED}) and oxidized (oxd773: oxidized in situ in air at 773 K for 60 min from RT at 10 K min^{-1} and cooled in the same flow to 473 K, ChI) samples before WGS test. Fig. 10b summarizes the treatments undergone by the catalysts in order to simulate the final conditions of the catalysts after a durability/regeneration test that involves a long exposition to the WGS atmosphere and start up/shut down cycles (ChII). Successively, in order to check the complete recovery of the catalysts, other two chemisorption experiments have been performed after an oxidation step (oxidized in situ in air at 773 K for 60 min and cooled in the same flow to 473 K) in between (ChIII and ChIV). The durability/regeneration test consists of a cycle of WGS (WGS1) followed by the steady-state durability test (in the WGS atmosphere for about 45 h), a second WGS cycle (WGS2) over the aged catalyst and a third cycle of WGS (WGS3) over in situ regenerated catalyst that was finally cooled in N_2 to RT.

Moreover, to evaluate separately the effects of the long-term exposure to the WGS atmosphere from those of start up/shut down cycles, the catalysts were treated as indicated in Fig. 10c, and the platinum dispersion of freshly aged catalysts (ChV) together with their in situ regenerated form (ChVI) were measured for comparison. These freshly aged catalysts were also investigated in parallel by HRTEM and TPD in He. All the chemisorption data are listed in Table 3. A CO chemisorption study carried over bare support $Ce_{0.56}Zr_{0.44}O_2$ treated in situ as oxd773 or red773 did not show any CO uptake, indicating no contribution from support in the catalysts investigated. Moreover, the viability of this CO pulse technique and choice of 473 K as the reduction temperature are supported by a previous study [43].

The correlation of the findings of CO chemisorption measurements and HRTEM are not straightforward. All the catalysts that underwent an in situ oxd773 treatment (ChI, ChIII, ChIV and ChVI) before the chemisorption measurement show the highest value of dispersion (14.8–48.4%) for a particular catalyst, and the active particle diameter obtained closely matches with that obtained from the HRTEM investigations (compare these values in Table 3 with the Pt crystallite size in Table 1). IWI(Cl) has the highest degree of dispersion of all the four catalysts. The activity order of the oxd773 catalysts is in conformity with the ChI dispersion values except the IWI(Cl) catalyst. Presence of a small amount of chloride can explain this. There is a negligible difference between ChIII and ChIV for a particular catalyst. Note that these two values correspond to two successive regeneration cycles and thus justify our regeneration procedure. These two values are also in corollary with ChVI values. Both the SCS catalysts have the similar dispersion values before the first cycle of WGS (ChI) and after regeneration (ChIII, ChIV and ChVI). But for the impregnated catalysts, there occurs a permanent loss of dispersion by 15–20% and is stabilized at that value afterwards. The aged catalysts (ChV) experience a significant loss of dispersion in the range 41–77% with respect to ChVI. The

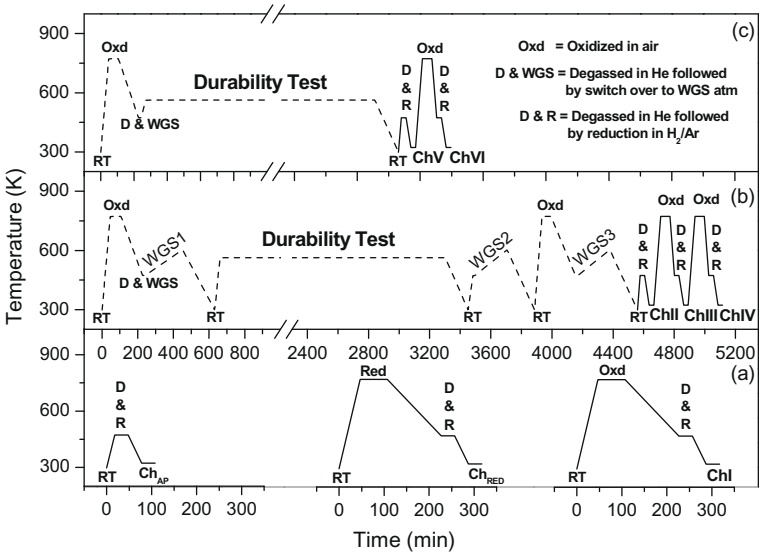

Fig. 10. Sequence of events indicating the state of catalyst before CO chemisorption measurement, (a) before ageing and (b and c) after ageing.

Table 3
CO chemisorption data on the catalysts following different treatments.[a]

Name of catalyst	Percent dispersion (active particle size, nm)							
	Ch_{AP}	Ch_{RED}	ChI	ChII	ChIII	ChIV	ChV	ChVI
CZ		0	0					
SCS(N)	12.1 (9.4)	8.6 (13.2)	25.8 (4.4)	13.8 (8.2)	26.6 (4.2)	28.5 (4.0)	9.7 (11.7)	26.8 (4.2)
SCS(Cl)	21.6 (5.2)	12.8 (8.8)	25.1 (4.5)	12.1 (9.3)	25.1 (4.5)	25.4 (4.5)	11.4 (9.9)	24.9 (4.5)
IWI(N)	14.8 (7.6)	11.7 (9.7)	18.6 (6.1)	6.3 (18.1)	14.7 (7.7)	15.6 (7.3)	3.5 (32.2)	16.3 (6.9)
IWI(Cl)	45.5 (2.5)	23.6 (4.8)	48.4 (2.3)	20.1 (5.6)	38.1 (3.0)	39.9 (2.8)	24.0 (4.7)	40.6 (2.8)

[a] For detail on treatments see text (Section 3.4) and Fig. 10.

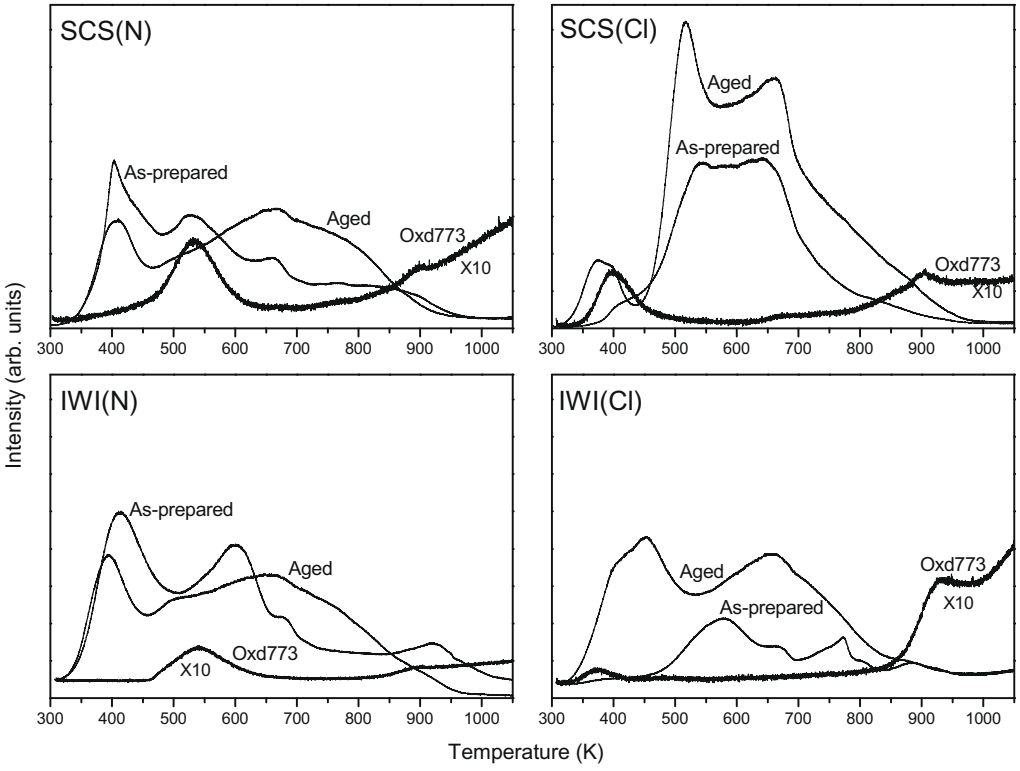

Fig. 11. Evolution of CO_2 during TPD in He of the catalysts in different forms.

loss of dispersion follows the following order: IWI(N)[79%] > SCS(N)[64%] ≈ SCS(Cl)[54%] > IWI(Cl)[41%]. Based on this, the shift activity is expected to be in the reverse order and in fact, the steady-state activity pattern follows it. The activity pattern of the regenerated catalysts is in corollary with the measured dispersion values.

Except for the SCS(N) catalyst, the dispersion value of the as-prepared catalyst, Ch_{AP}, is lower by 6–20% than the corresponding ChI values. It is noted that even the red773 treatment also leads to very low dispersion values, Ch_{RED}, lower than the Ch_{AP} values.

The drop in dispersion cannot be accounted for by a decrease in surface area, because the catalysts are found to be stable in the reformate mixture. So, there can be a sintering of Pt particles, or they are covered by an irreversibly adsorbed species [17]. Since a H_2/Ar mixture has been used to reduce the catalysts before CO chemisorption, a component in the reformate mixture other than hydrogen (CO, CO_2 or H_2O) contributes to the loss of dispersion.

3.5. Temperature-programmed desorption studies

Fig. 11 shows the evolution of CO_2 liberated from the decomposition of carbonate species deposited on the surface of the four catalysts in the as-prepared, oxd773 (treated in situ in air for 60 min) and aged forms when they were desorbed in He flow from RT to 1073 K. The TPD profiles indicate presence of carbonate species in both the as-prepared and aged catalysts. Desorption of the carbonate species of the aged catalysts starts in the beginning itself and is consisted of mainly two peaks, one, in the range 380–450 K, and the other, at around 670 K (except for SCS(Cl) where it is lower by ca.70 K). The intensity of the first peak is low, and it is narrow, whereas the second peak is very broad and tails off beyond 800 K. This first peak can be assigned to weakly adsorbed carbonate species, and the second peak then corresponds to strongly chemisorbed carbonate species. The highest amount of carbonate is formed over the SCS(Cl) catalyst, and it is similar for the other three catalysts. Thus, formation of carbonate is less important as the cause for decay in activity during durability test, rather, the sintering/embedding effect plays the major role. Our regeneration treatment at 773 K almost entirely covers the desorption region and is certainly sufficient to remove the deposited carbonate.

The overall intensity of the CO_2 desorption profiles of the as-prepared catalysts were lower when compared to the aged catalysts, and the second peak was situated at further lower temperatures. Both the catalysts from chloride precursor hardly show peaks due to weakly adsorbed surface carbonates. The lowest amount of carbonate was found in the IWI(Cl) catalyst. Thus, in the freshly prepared samples, a certain amount of carbonate accumulates in contact with air during the course of preparation. When these catalysts are treated in situ as oxd773 before TPD is performed, the carbonate peaks disappeared as evidenced from the negligible intensity profiles. So, there is no carbonate layer over the samples before the durability test, and it is only formed as a result of exposure of the catalysts to the simulated mixture employed for WGS activity.

4. Discussion

We have motivated our interest in this work to understand the different behaviour of the direct combustion-synthesized catalysts with respect to the corresponding impregnated catalysts employing two commonly used precursors of platinum, namely, nitrate and chloride. The support, which has been prepared by combustion synthesis, is similar for all the catalysts, and this enabled us to explore the influence of methodology as well as precursor of platinum on its dispersion and interaction with the support for water gas shift reaction. The dispersion of Pt is similar for the SCS catalysts (about 25%); thus, the one-step solution combustion method produces a reasonably highly dispersed catalyst, despite the modest surface area values. The transient nature of combustion together with the evolution of large amount of gases makes this possible. The transient high temperature contributes to high crystallinity, and the presence of all the reactants (oxidizers and reducer) in solution phase ensures the homogeneity. Therefore, by combustion synthesis, it is possible to obtain catalysts with a desired and reproducible metal loading and a defined level of dispersion that depends only marginally on the type of precursors used. It is difficult to obtain such a level of homogeneity and dispersion following the incipient wetness technique as it is shown for the IWI(N) catalyst. In fact, with this technique, the final result depends on several parameters such as the type of support, the kind and concentration of precursor solution and the modality of drying. These factors are not always easy to optimize. It is worthy to note that in this type of synthesis, the final dispersion is correlated with the nature of precursors. In our synthesis conditions, the IWI(Cl) catalyst prepared using chloride precursor shows a higher dispersion than IWI(N) and the best dispersion of all the catalysts examined. The reason for these differences in metal dispersion using nitrate or chloride precursors could be due to the formation of oxo-chlorinated species that interact favourably with the support hindering growth of Pt particles. It was found that there is a relationship between the inhibitory effect of Pt sintering and the possibility to keep the Pt in oxidized state through a strong interaction with the support [44]. In the past, we observed opposite results with the use of chloride and nitrate precursors [25]. The reason of these controversial outcomes could be due to a different modality of impregnation. In this case, we preferred to impregnate the support in one-step with equal volumes of solution of the nitrate and chloride salts of platinum for the sake of similarity. But since the solubility of the $Pt(NH_3)_4(NO_3)_2$ in water is less than that of H_2PtCl_6, complete dissolution of the former was achieved by slight warming. In our previous reports, we impregnated the support in more steps dissolving the nitrate salt at room temperature using larger volume of water. This suggests that in the incipient wetness impregnation technique, concentration of solution and successive drying step affect the final dispersion of the metal. Moreover, it is not excluded that the composition and surface area of support could play a role in the dispersion determined by a specific precursor. The lower uniformity of metal dispersion in the case of IWI catalysts in comparison to the SCS catalysts can be inferred also from the different agreement between XRD and HRTEM characterization for the two types of catalysts. For combustion-synthesized samples, XRD and HRTEM results are in agreement indicating a fine and homogeneous distribution of platinum. On the contrary, the findings about the size of Pt crystallites from XRD studies of the IWI catalysts are not in accordance with the respective HRTEM findings. While XRD suggests the presence of some bigger Pt crystallites, the HRTEM images of the catalyst do not show any big crystallite of Pt. This is because the large Pt particles are opaque to the electron beam owing to their high electron density and hence escape HRTEM analysis. However, since XRD is a bulk technique, a few big platinum crystallites can be responsible for an intense platinum metal signal in the XRD pattern. This does not necessarily depict the overall picture of the catalyst material. Therefore, the impregnation brings about the formation of small crystallites together with larger particles showing less uniformity in the particle size of platinum in comparison to the catalyst prepared by combustion synthesis.

Distribution of Pt before and after ageing as revealed by HRTEM investigations did highlight the following aspects. First, both the SCS catalysts experience a marginal sintering effect on ageing in the WGS atmosphere (Pt crystallite size increases from 3.8–3.6 nm

in the oxd773 catalyst to 4.1–4.0 nm in the aged catalyst) with concomitant broadening of distribution. Thus, although the mean size increases, a larger number of Pt particles do have similar size in the aged catalysts than in the oxidized catalysts. Second, for the impregnated catalysts, on the contrary, the platinum distribution remains essentially constant for both before and after the ageing with a slight increase of Pt size in the aged catalyst from chloride precursor.

The differences in activity observed in AP, red773 and oxd773 forms of the SCS catalysts can be correlated with their different microstructure. HRTEM reveals the occurrence of an epitaxial relationship between the support and metal particles in the fresh and in the reduced SCS catalyst prepared from nitrate precursor. It is well known that epitaxial relationship between the support and metal particles induces structural strain, both in the metal particles and in the metal metal-oxide interface [45]. It is reported that strain of metal surfaces is correlated with adsorption energies and activation energy barriers of the metals, and this effect is due to a shift in the position of the center of the metal *d* bands respect to the Fermi level [46]. We can suppose that in the present case, structural strain in such small Pt particles likely results in a strong adsorption of reactants, which, in turn, could explain the lower observed activity. However, the role of epitaxial bonding in the activity and stability of these catalysts is difficult to elucidate at this point of our investigations, and further studies will be necessary to fully address this issue. In addition, there is also a thermal effect (773 K for 1 h) in the reduced and oxidized forms of both the SCS catalysts that is absent in their as-prepared forms. In general, the thermal effect positively influences the SCS catalysts as it is clear from the higher activity of red773 and oxd773 catalysts over the corresponding as-prepared catalysts. These thermal treatments result in changes in the microstructure. The oxidative treatment in SCS(N) leads to a catalyst state with highest activity since it removes the epitaxy in the structure but does not disrupt the homogeneity of Pt distribution. Only a little decrease of average particle size was observed after the treatment. On the other side, the oxidative treatment paves the way towards a more homogeneous distribution with concomitant lowering of average Pt crystallite size in SCS(Cl). The reductive treatment is not sufficient to break the epitaxy in the SCS(N) catalyst, while it leads to an inhomogeneous distribution of Pt in SCS(Cl) catalyst. The resulting effect is a lower activity of the red773 catalysts compared to the oxd773 catalysts. For the impregnated catalysts, on the contrary, no such differences in activity are observed since the preparation step of these catalysts involves calcination in air at 823 K for 1 h. The presence of chloride in SCS(Cl) is responsible for its lower activity compared to SCS(N) in each of the three forms.

The much lower value of dispersion obtained for SCS(N) catalyst in as-prepared (53% lower than ChI) and red773 forms (67% lower than ChI) can also be explained on the basis of epitaxy in the structure [40,41]. On the contrary, the HRTEM images show no occurrence of epitaxy in the microstructure of the as-prepared and reduced catalysts of SCS(Cl), but the particle size distribution in these two forms is more heterogeneous (2–7 nm) than in the other samples and explains the lower dispersion values. Both the SCS catalysts in oxd773 form do not show epitaxial relationship, and they exhibit the highest dispersion values. In addition, the sample preparation step before chemisorption (involving degassing in He at 473 K) is able to remove the weakly adsorbed surface carbonates (as clear from the TPD profiles) from the as-prepared and aged samples but do not affect those strongly adsorbed; this lowers the CO adsorption capability thus affecting metal dispersion values.

Another point of interest in this study is that the nature of deactivation depends on the technique of deposition and on the nature of precursors. The ex-chloride catalysts are less deactivated or not deactivated in the reformate atmosphere, whereas the ex-nitrate catalysts are more prone to deactivation. For both ex-nitrate and ex-chloride SCS catalysts, the deactivation occurred in the first hours, then the activity was stabilized to a constant value. The main causes of deactivation could be correlated with the accumulation of carbonate species as evidenced by TPD measurements on the aged catalysts and/or the change in the distribution of platinum particle size mentioned above. It is difficult to discriminate between these two effects. Since the average size of Pt being similar in both the SCS catalysts after ageing, the higher tendency to carbonate formation of the SCS(Cl) catalyst is responsible for its higher deactivation than SCS(N) catalyst. However, the deactivation is completely reversed by an oxidizing treatment at 773 K. This indicates that along with the removal of adsorbed carbonate species, there is also a reversible switching between the two distribution patterns as can be inferred from the complete recovery of dispersion values. Alternatively, we could conclude that the slight sintering of metal does not affect much the activity of the catalyst.

For the IWI(N) catalyst, no sintering effect is visible by HRTEM, but an additional effect of strong embedding by support is present together with the formation of carbonates. The strong embedding of the active phase by the support in this catalyst reduces the exposed platinum area for CO adsorption leading to a catalyst with decreased activity. This effect is so critical that even the oxidative treatment at 773 K is not enough to regenerate the catalyst to its initial state. The lower value of dispersion of the regenerated catalyst supports this.

The most interesting behaviour is shown by the impregnated catalyst from the chloride precursor. In general, it is reported in the literature that the presence of chloride in the sample reduces the activity acting as a poison. In the case of ceria-based catalysts, the presence of chloride ions dramatically reduces the oxygen-spillover and back-spillover rates by forming CeOCl species on the ceria support [47]. Formation of this CeOCl species decreases the number of available hydroxyl groups that were claimed to be one key parameter responsible for the possible migration of chemisorbed oxygen species and/or formation of formate intermediates in the WGS activity. Duprez and coworkers [48] reported a sharp decrease in CO conversion in PROX in the case of the catalyst prepared from H_2PtCl_6 precursor. In fact, there is a positive gain in activity for the impregnated catalyst from the chloride precursor during or after the long-term durability test. This is partly due to the removal of residual chlorides during the reaction as it is confirmed from the analysis of the amount of chloride before and after the durability test (see Table 1). We suppose that the chlorides are stripped off by their reaction with water to form HCl via a mechanism similar to what described by Paulis et al. [49]. This fact could explain the enhancement of activity of IWI(Cl) sample; however, there are still a few points that need to be clarified and particularly (i) the activity pattern of IWI(Cl) catalyst presents two steps suggesting that the mechanism of activation might involve more than one single process and (ii) the different behaviour of IWI(Cl) and SCS(Cl) catalysts may result from processes other than loss of chloride during reaction. It is evident from the above considerations that these results are the effect of the interplay between different processes that contribute positively and negatively to overall catalytic activity. The presence of chlorine has certainly a negative effect on activity; chloride ions fill the oxygen vacancies close to the platinum interface blocking the active sites and affecting the spillover and back-spillover rate of reactants. Moreover, the adsorption capability of platinum could be inhibited, as platinum atoms at the metal support interface could behave as a partially oxidized center with a lower electron density [50]. We have shown that during the durability test, chlorine is removed from both Cl-containing samples; water vapour present in the stream is likely involved in this process [49]. Sintering of Pt particles is another phenomenon that

occurs during reaction. We have recently reported that very small Pt particles have generally a reduced WGS activity with respect to larger particles [25]. The reasons of these findings are at the moment unclear. However, for the catalysts investigated here, particle size of ca. 3 nm seems to be the optimum size for activity. Therefore, an increase/decrease of activity is observed when sintering involves particles smaller/larger than 3 nm, and this could explain why sintering in IWI(Cl) and in SCS(Cl) could have opposite effects. Formation of carbonate is also a well-known deactivation mechanism in WGSR [51]. It is reported that carbonate formation is influenced negatively by the presence of a large amount of chloride that adsorbs competitively on Ce^{3+}sites [52]. Therefore, the different amounts of carbonate present on each catalyst (see Fig. 11) and a different dynamic of their formation could introduce another difference in the deactivation/activation profiles of the two catalysts.

Summing up, the phenomena involved in the deactivation/activation processes of ex-chloride samples are mainly (i) removal of chlorine by water, (ii) chemisorption of CO_2 and formation of carbonates, and (iii) sintering of Pt particles. While in IWI(Cl), the occurrence of these phenomena results in an overall gain of activity during time on stream, in SCS(Cl) catalysts, the positive effect due to the strip off of chlorine by water is more than compensated by the negative effect of formation of carbonate and growth of the dimension of Pt particles.

5. Conclusions

We have reported a single-step, combustion approach to prepare an effective and durable WGS catalyst. The high dispersion of platinum coupled with the high crystallinity of the combustion-synthesized catalyst makes it a potential candidate in parallel with the conventional impregnated catalysts for the WGS reaction at high space velocities. The SCS catalysts are sensitive to the pretreatment atmosphere. Oxidation at mild temperature activates both ex-nitrate and ex-chloride samples. In the former catalysts, the oxidation removes the epitaxial bonding between Pt particles and support, which is responsible for the lower activity of fresh catalyst. The degrees of deactivation of different catalysts and underlying causes can be envisaged in relation to the method of preparation and the precursors used. The activity of SCS catalysts can be recovered completely after ageing, while deactivation of the impregnated catalyst from nitrate precursor IWI(N) is not reversible under similar conditions. On the contrary, the impregnated catalyst from chloride precursor shows higher activity after ageing. Removal of chlorides during durability test and long-term stabilization of Pt crystallite size at ~3 nm are responsible for this activity enhancement.

Acknowledgments

The authors thank MIUR and Regione Friuli Venezia Giulia for support through PRIN project and Progetti LR 26/05 and MICINN for support through project CTQ2009-12520.

References

[1] R. Farrauto, S. Hwang, L. Shore, W. Ruettinger, J. Lampert, T. Giroux, Y. Liu, O. Ilinich, Annu. Rev. Mater. Res. 33 (2003) 1.
[2] C. Ratnasamy, J. Wagner, Catal. Rev. Sci. Eng. 51 (2009) 325.
[3] A.S.K. Hashmi, G.J. Hutchings, Angew. Chem. Int. Ed. 45 (2006) 7896.
[4] R. Burch, Phys. Chem. Chem. Phys. 8 (2006) 5483.
[5] A. Luengnaruemitchai, S. Osuwan, E. Gulari, Catal. Commun. 4 (2003) 215.
[6] T. Bunluesin, R.J. Gorte, G.W. Graham, Appl. Catal. B: Environ. 15 (1998) 107.
[7] I.D. González, R.M. Navarro, M.C. Álvarez-Galván, F. Rosa, J.L.G. Fierro, Catal. Commun. 9 (2008) 1759.
[8] P. Panagiotopoulou, D. I Kondaries, J. Catal. 225 (2004) 327.
[9] D. Tibiletti, F.C. Meunier, A. Gouget, D. Reid, R. Burch, M. Boaro, M. Vicario, A. Trovarelli, J. Catal. 244 (2006) 183.
[10] P.O. Graf, D.J.M.D. Vlieger, B.L. Mojet, L. Lefferts, J. Catal. 262 (2009) 181.
[11] S. Ricote, G. Jacobs, M. Milling, Y. Ji, P.M. Patterson, B.H. Davis, Appl. Catal. A 303 (2006) 35.
[12] R. Radhakrishnan, R.R. Willigan, Z. Dardas, T.H. Vanderspurt, AIChE J. 52 (2006) 1888.
[13] P.S. Querino, J.R.C. Bispo, M.d.C. Rangel, Catal. Today 107–108 (2005) 920.
[14] D.C. Grenoble, M.M. Estadt, D.F. Ollis, J. Catal. 67 (1981) 90.
[15] Y. Lei, N.W. Cant, D.L. Trimm, Catal. Lett. 103 (2005) 133.
[16] P. Panagiotopoulou, D.I. Kondarides, Catal. Today 112 (2006) 49.
[17] P. Panagiotopoulou, J. Papavasiliou, G. Avgouropoulos, T. Ioannides, D.I. Kondarides, Chem. Eng. J. 134 (2007) 16.
[18] F. Dong, A. Suda, T. Tanabe, Y. Nagai, H. Sobukawa, H. Shinjoh, M. Sugiura, C. Descorme, D. Duprez, Catal. Today 93–95 (2004) 827.
[19] W. Ruettinger, X. Liu, R.J. Farrauto, Appl. Catal. B: Environ. 65 (2006) 135.
[20] A. Goguet, R. Burch, Y. Chen, C. Hardacre, P. Hu, R.W. Joyner, F.C. Meunier, B.S. Mun, D. Thompsett, D. Tibiletti, J. Phys. Chem. C 111 (2007) 16927.
[21] X. Liu, W. Ruettinger, X. Xu, R. Farrauto, Appl. Catal. B: Environ. 56 (2005) 69.
[22] W. Deng, M. Flytzani-Stephanopoulos, Angew. Chem. Int. Ed. 45 (2006) 2285.
[23] S.Y. Choung, M. Ferrandon, T. Krause, Catal. Today 99 (2005) 257.
[24] R. Radhakrishnan, R.R. Willigan, Z. Dardas, T.H. Vanderspurt, Appl. Catal. B: Environ. 66 (2006) 23.
[25] M. Boaro, M. Vicario, J. Llorca, C.d. Leitenburg, G. Dolcetti, A. Trovarelli, Appl. Catal. B: Environ. 88 (2009) 272.
[26] D. Pierre, W. Deng, M. Flytzani-Stephanopoulos, Top. Catal. 46 (2007) 363.
[27] P. Bera, S. Malwadkar, A. Gayen, C.V.V. Satyanarayana, B.S. Rao, M.S. Hegde, Catal. Lett. 96 (2004) 213.
[28] S.T. Aruna, K.C. Patil, NanoStruct. Mater. 10 (1998) 955.
[29] S. Colussi, A. Gayen, M. Farnesi Camellone, M. Boaro, J. Llorca, S. Fabris, A. Trovarelli, Angew. Chem. Int. Ed. 48 (2009) 8481.
[30] E. Aneggi, M. Boaro, C. de Leitenburg, G. Dolcetti, A. Trovarelli, J. Alloys Compd. 408–412 (2006) 1096.
[31] G. Colon, F. Valdivieso, M. Pijolat, R.T. Baker, J.J. Calvino, S. Bernal, Catal. Today 50 (1999) 271.
[32] G. Zhou, P.R. Shah, T. Kim, P. Fornasiero, R.J. Gorte, Catal. Today 123 (2007) 86.
[33] H. Vidal, J. Kaspar, M. Pijolat, G. Colon, S. Bernal, A. Cordon, V. Perichon, F. Fally, Appl. Catal. B 27 (2000) 49.
[34] M. Hirano, A. Suda, J. Am. Ceram. Soc. 86 (2003) 2209.
[35] A.C. Larson, R.B. van Dreele, General Structural Analysis (GSAS), Los Alamos National Laboratory Report LAUR 86-748, 2000.
[36] B.H. Toby, J. Appl. Crystallogr. 34 (2001) 210.
[37] J.R. Ladebek, J.P. Wagner, in: W. Vielstich, H.A. Gasteiger, A. Lamm (Eds.), Handbook of Fuel Cells Fundamentals Technology and Applications, "Catalytic Development for Water-Gas Shift", Wiley, 2003, pp. 191–201.
[38] S. Rossignol, Y. Madier, D. Duprez, Catal. Today 50 (1999) 261.
[39] A. Trovarelli, M. Boaro, E. Rocchini, C. de Leitenburg, G. Dolcetti, J. Alloys Compd. 323–324 (2001) 584.
[40] S. Bernal, J.J. Calvino, M.A. Cauqui, J.M. Gatica, C. Larese, J.A. Pérez Omil, J.M. Pintado, Catal. Today 50 (1999) 175.
[41] J.M. Gatica, R.T. Baker, P. Fornasiero, S. Bernal, J. Kaspar, J. Phys. Chem. B 105 (2001) 1191.
[42] H. Idriss, M. Scott, J. Llorca, S.C. Chan, W. Chiu, P.Y. Sheng, A. Yee, M.A. Blackford, S.J. Pas, A.J. Hill, F.M. Alamgir, R. Rettew, C. Petersburg, S. Senanayake, M.A. Barteau, ChemSusChem 1 (2008) 905.
[43] T. Takeguchi, S. Manabe, R. Kikuchi, K. Eguchi, T. Kanazawa, S. Matsumoto, W. Ueda, Appl. Catal. A: Gen. 293 (2005) 91.
[44] Y. Nagai, T. Hirabayashi, K. Dohmae, N. Takagi, T. Minami, H. Shinjoh, S. Matsumoto, J. Catal. 242 (2006) 103.
[45] N. Barrabés, K. Föttinger, A. Dafinov, F. Medina, G. Rupprechter, J. Llorca, J.E. Sueiras, Appl. Catal. B: Environ. 87 (2009) 84.
[46] M. Mavrikakis, B. Hammer, J.K. Nørskov, Phys. Rev. Lett. 81 (1998) 2819.
[47] D.I. Kondarides, X.E. Verykios, J. Catal. 174 (1998) 52.
[48] A. Wootsch, C. Descorme, D. Duprez, J. Catal. 225 (2004) 259.
[49] M. Paulis, H. Peyrard, M. Montes, J. Catal. 199 (2001) 30.
[50] E. Marceau, H.L. Pernot, M. Che, J Catal. 197 (2001) 394.
[51] C.H. Kim, L.T. Thompson, J. Catal. 230 (2005) 66.
[52] A. Holmgrem, B. Andersson, D. Duprez, Appl. Catal. B: Environ. 22 (1999) 215.